



## Computational catalysis

Mechanistic insights into the double C–H (de)activation route of a Ru-based olefin metathesis catalyst<sup>☆</sup>Albert Poater, Luigi Cavallo<sup>\*</sup>

Department of Chemistry, University of Salerno, via Ponte don Melillo, Fisciano I-84084, Italy

## ARTICLE INFO

## Article history:

Available online 21 February 2010

## Keywords:

Homogeneous catalysis  
Olefin metathesis  
Computational catalysis  
Reaction mechanisms

## ABSTRACT

A theoretical study of a double C–H activation mechanism that deactivates a family of second-generation Ru-based catalysts is presented. DFT calculations are used to rationalize the complex mechanistic pathway from the starting precatalyst to the experimentally characterized decomposition products. We thoroughly study all intermediates proposed by Grubbs and co-workers, characterizing them with different computational tools as aromaticity and Mayer Bond Order. In particular, we show that all the intermediates proposed by Grubbs and co-workers are indeed possible intermediates of the deactivation pathway, although the sequence of steps is somewhat different. Finally, we reveal why free PCy<sub>3</sub> is fundamental to shift the equilibrium towards double C–H activation.

© 2010 Elsevier B.V. All rights reserved.

## 1. Introduction

Ru-based catalysts for olefin metathesis have acquired a prominent role in modern organic synthesis [1], and are expanding their area from lab scale to industrial production. This step forward requires that very active and stable catalysts have to be designed. Along this direction, replacement of a phosphane ligand with a N-heterocyclic carbene (NHC) ligand in Grubbs 1st generation catalysts [2] lead to NHC-based 2nd generation catalysts that proved more active and in many cases even more stable [3]. The origin of the greater activity of NHC-based catalysts is now rather well understood [4] and, although still incomplete [5,6], this knowledge is currently used to approach the ambitious “rational design” of new catalysts. Unfortunately, stability remains an issue, and very little is known about deactivation pathways [7]. Recently several studies have revealed that the presence of  $\pi$ -acids are another way to promote deactivation reactions which are now reasonably understood, although this deactivation mechanism is not operative in standard metathesis conditions [8]. On the other hand, in one case, detailed experiments have characterized the deactivation products of a typical olefin metathesis catalyst [7f], which opened the route to the rationalization of catalysts deactivation under metathesis conditions, see Scheme 1.

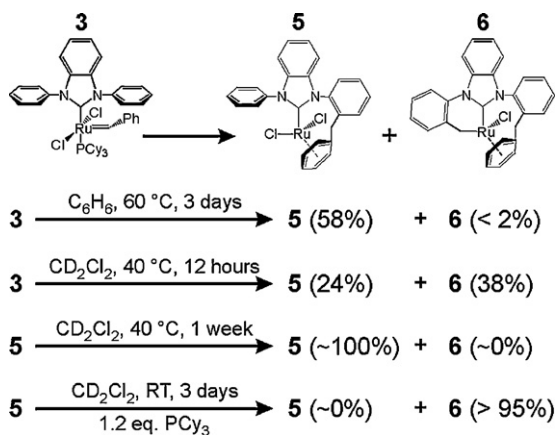
Precatalyst **3** heated in benzene at 60 °C under inert condition decomposes to complex **5** after 3 days (58% yield) with traces of complex **6** (see Scheme 1). Replacing benzene with CD<sub>2</sub>Cl<sub>2</sub> leads

to much faster decomposition. However, after 12 h at 40 °C the main decomposition product is **6** (38% yield), while **5** is the minor decomposition product (24% yield). Complexes **5** and **6** were fully characterized by X-ray crystallography [7f].

Experiments also revealed that complex **5** is stable at 40 °C for a week, while it evolves to complex **6** at RT in only 3 days if PCy<sub>3</sub> is added to reaction media. This suggested that **5** is a precursor of **6**, and that activation of the *ortho*-C–H bond of a N-phenyl ring of the NHC-ligand likely is the first step. On this basis, the deactivation mechanism shown in Scheme 2 was proposed [7f]. Intermediates **8** and **9** are only hypothetical species along the deactivation pathway, since no intermediates could be characterized. A recent theoretical study revealed that the intermediates proposed by Grubbs, with the exception of intermediate **8**, are energetically feasible, and showed that the flexibility of the phenyl groups of the N-heterocyclic carbene plays the most important role in the initiation and also in the propagation of the reaction [7m].

Assisted by DFT calculations we propose here a complete theoretical characterization of this deactivation mechanism. To allow for an easy comparison with the experimental paper, we denote species that were described in the experimental paper with the same labels, see Scheme 2. We show here that **8** and **9** are indeed intermediates along the deactivation pathway, and that **5** is a precursor of **6**. However, we also think that **9** could precede **8**, rather than follow it. Basically, we will extend the work of Suresh and co-workers to include a low energy pathway for formation of the second deactivation product **6**, clarifying the fundamental role of PCy<sub>3</sub> to promote this step. Further, we will perform a thorough characterization of the various intermediates using standard analysis tools such as aromaticity and Mayer Bond Orders (MBO).

<sup>☆</sup> This paper is part of a special issue on Computational Catalysis.<sup>\*</sup> Corresponding author.E-mail address: [lcavallo@unisa.it](mailto:lcavallo@unisa.it) (L. Cavallo).



Scheme 1.

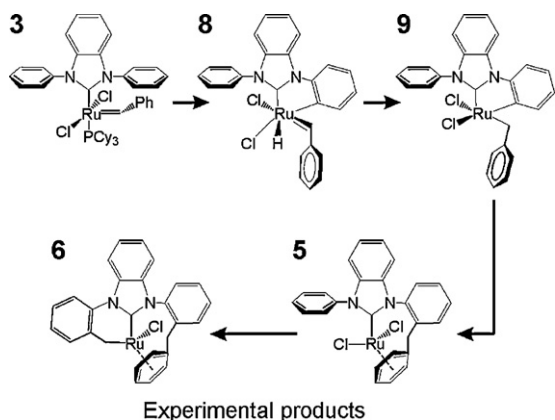
## 2. Computational details

All the density functional theory (DFT) calculations were performed using the Gaussian03 package [9]. The BP86 GGA functional of Becke and Perdew was used [10]. The SVP triple- $\zeta$  basis set with one polarization function was used for main group atoms [11], while the relativistic SDD effective core potential in combination with a triple- $\zeta$  basis set was used for the Ru atom [12]. All geometries were verified by frequency calculations that resulted in 0 and 1 imaginary frequency for intermediates and transition states, respectively. The reported energies include the vibrational gas-phase zero-point energy term, and a solvation term that was obtained through single-point calculations on the gas-phase optimized geometries. The polarizable continuous solvation model IEF-PCM as implemented in the Gaussian03 package has been used [13].  $\text{CH}_2\text{Cl}_2$  was chosen as model solvent, with a dielectric constant  $\epsilon = 8.93$ . Standard non-electrostatic terms were also included.

The strength of the main bonds was evaluated with the Mayer Bond Order (MBO) [14], which is a valuable tool in the analysis of the bonding in main group compounds and has been also used to characterize transition metal systems [15,16].

Finally, in some cases we discuss the change in the local aromaticity of a given ring. As a structure-based measure, we have used the Kruszewski and Krygowski harmonic oscillator model of aromaticity (HOMA) index; see Eq. (1) [17]:

$$\text{HOMA} = 1 - \frac{\alpha}{n} \sum_{i=1}^n (R_{\text{opt}} - R_i)^2 \quad (1)$$



Scheme 2.

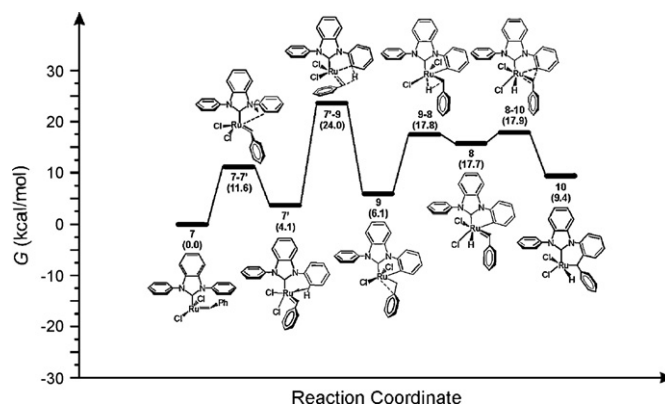


Fig. 1. First part of the deactivation pathway.

where  $n$  is the number of bonds considered,  $R_i$  are the bond lengths, and  $\alpha$  is an empirical constant (for C–C bonds  $\alpha = 257.7$ ) fixed to give HOMA = 0 for a model nonaromatic system and HOMA = 1 for a system with all the bonds equal to their optimal value  $R_{\text{opt}}$ , which is 1.388 Å for C–C bonds (i.e., the bond length in fully aromatic systems).

## 3. Results and discussion

The first part of the deactivation intermediate, from the naked 14e species **7** to the intermediate **10** is shown in Fig. 1. The first step of the deactivation path starts from complex **7** (formed by phosphane dissociation from **3**, which costs 16.6 kcal/mol) and leads to complex **6**. The electron-deficient 14-electron species **7** can engage one of the *ortho*-C–H bonds of a N-phenyl ring of the NHC-ligand into a rather stable agostic interaction through transition state **7–7'** and a barrier of 11.6 kcal/mol. The resulting intermediate **7'**, which is 4.1 kcal/mol higher in energy than **7**, is a text-book example of agostic complexes, with a clearly elongated C–H bond, 1.17 Å with respect to 1.10 Å in **7**, and a Ru–C–H angle of only 53.3°. A three dimensional representation of the structures, with selected distances, is reported in Fig. 2.

The next step is an oxidative addition consisting in the transfer of the agostic hydrogen of **7'** to the nearby  $\alpha$ -C atom of the benzylidene group, through transition state **7'–9** and a barrier of 19.9 kcal/mol, to reach intermediate **9**, in which the benzylidene group is transformed into a benzyl group, and the Ru atom forms a new  $\sigma$ -bond with the *ortho*-C atom of the N-phenyl ring of NHC-ligand involved in the agostic interaction. Intermediate **9**, originally suggested by Grubbs and co-workers, is 6.1 kcal/mol higher in energy than **7**, and it is stabilized by an interaction between the Ru atom and the *ipso*-C atom of the benzyl group.

The other key intermediate proposed by Grubbs and co-workers, the Ru-hydride species **8**, is reached from **9** via the transfer of a  $\alpha$  hydrogen from the benzyl group to the Ru atom through transition state **9–8** and a barrier of 11.7 kcal/mol. This H-transfer step restores the benzylidene group in **8**. Intermediate **8**, 17.7 kcal/mol above **7**, is rather unstable since the newly formed benzylidene group can insert into the  $\sigma$ -bond between the Ru atom and the *ortho*-C atom of the N-phenyl ring of NHC-ligand through transition state **8–10** and the almost negligible barrier of 0.2 kcal/mol only. The Ru-hydride intermediate **10**, which is 9.4 kcal/mol above **7**, was not postulated by Grubbs and co-workers, and it is the only additional “chemically different” piece that is needed to connect **7–5** and **6**.

The second part of the deactivation intermediate, from intermediate **10** to the experimentally characterized products is shown in Fig. 3. Intermediate **10** can evolve through transition **10–5'''** and a

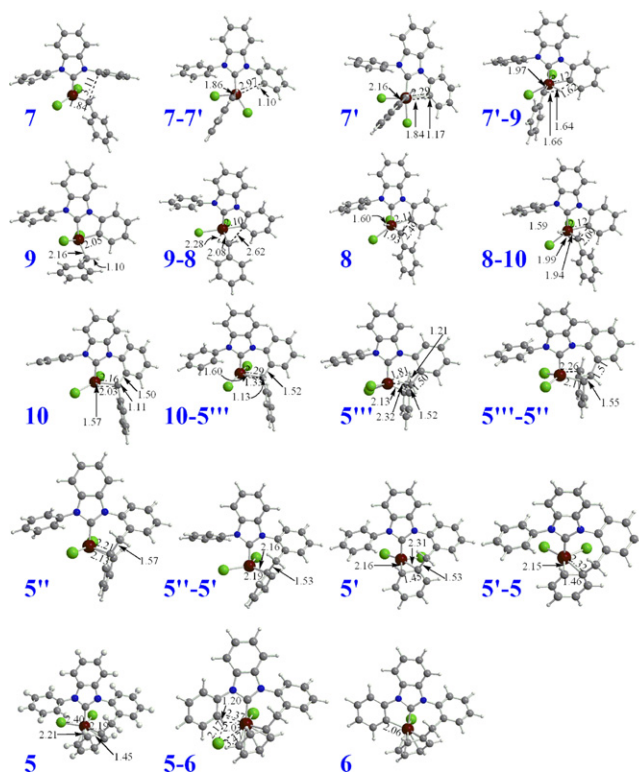


Fig. 2. Optimized structures of the deactivation pathway, with selected distances, in Å.

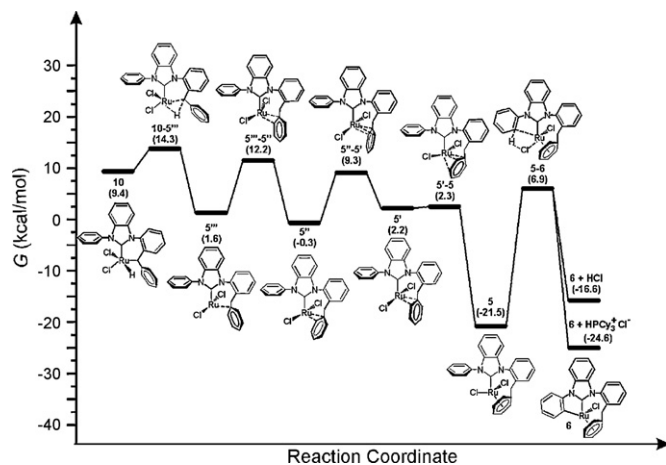


Fig. 3. Second part of the deactivation pathway.

barrier of 5.9 kcal/mol to intermediate  $5''$ . This reductive elimination step breaks the Ru–hydride bond. Intermediate  $5''$ , which is 1.6 kcal/mol above  $7$ , is stabilized by a strong interaction with the *ipso*-C atom of the Ph group of the formerly benzylidene moiety [18]. Intermediate  $5''$  is only a kinetic intermediate to the decomposition product  $5$ , which can be reached from  $5''$  through a series of haptotropic shifts that involve the Ru atom and the Ph group of the formerly benzylidene moiety. The remarkable stability of product  $5$ , 21.5 kcal/mol below the starting species  $7$ , probably is the key to understand why in a previous theoretical study intermediates  $5''$ ,  $5'$ , and  $5'$  were not located [7m]. However, the barriers separating  $5''$  from  $5'$ , and  $5'$  from  $5'$ , about 10 kcal/mol, are not negligible, and underline the complexity of this deactivation pathway.

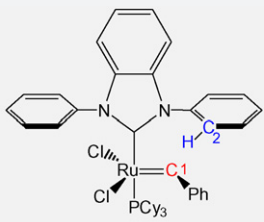
Finally, one of the Cl atoms of  $5$  can interact with an *ortho*-H atom of the other N-phenyl ring of the NHC-ligand to eliminate

one HCl molecule, through transition state  $5-6$  and a barrier of 28.4 kcal/mol, to yield the other observed decomposition product,  $6$ . Complex  $6 + \text{HCl}$  is 4.9 kcal/mol higher in energy than  $5$ . On the other hand, if the extracted HCl molecule is trapped by a  $\text{PCy}_3$  molecule, the resulting product  $6 + [\text{HPCy}_3^+][\text{Cl}^-]$  is 3.1 kcal/mol below  $5$ , which is in qualitative agreement with the experimental finding that  $5$  is thermodynamically stable unless a Lewis base such  $\text{PCy}_3$  is added, which shifts the equilibrium towards  $6$  [19]. The key role of  $\text{PCy}_3$ , indicated by our calculations for the first time, allows to improve the comprehension of the higher stability of complex  $6$  with respect to  $5$  [7m].

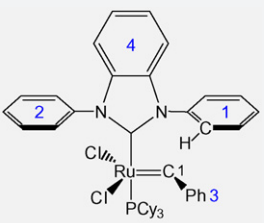
The decomposition pathway discussed so far is the one that seems to be preferred according to our calculations. Of course, we also tested other possibilities. For example, we started with the  $7 \rightarrow 8 \rightarrow 9$  pathway postulated by Grubbs and co-workers. However, transition state  $7'-8$ , which corresponds to a direct transfer of the *ortho*-H atom from the N-phenyl ring of the NHC-ligand to the Ru atom, and that connects  $7'$  to  $8$  in a single step, was found to be 7.9 kcal/mol above transition state  $7'-9$ , which rules out the  $7 \rightarrow 8 \rightarrow 9$  pathway in favor of the  $7 \rightarrow 9 \rightarrow 8$  pathway. Similarly, we tested if  $9$  can be directly transformed into one of the haptotomers of  $5$ . If feasible, this step would simplify the decomposition pathway by removing intermediate  $8$ . However, the best transition state we found,  $9-5''$ , is 14.3 kcal/mol higher in energy than transition state  $9-8$ , which suggests that  $8$  is a real intermediate along the decomposition pathway. The high barrier for the  $9-5''$  step is in agreement with the results of Suresh and co-workers [7m], but it also demonstrates that the pathway supported by our calculations is probably a better description of the experimentally followed pathway.

The Mayer Bond Orders (MBO) reported in Table 1 display the evolution of the most relevant bonds formed or broken during the deactivation process. In Table 1 we include the main MBO related to the first deactivation process leading to complex  $5$ . The phenylidene carbon bonded to the ruthenium decreases its strength from a nearly formal double bond in species  $3$  with a MBO of 1.675 to a somewhat simple bond in intermediate  $10$  with MBO of 0.857, disappearing almost completely in  $5'$ . Meanwhile, the first deactivation step implies the interaction of the Ru center with one of the *ortho*-C atoms of a phenyl N-substituent in intermediate  $9$ , and the MBO analysis with a value for the Ru–C(2) bond of 0.950 in  $9$ , characterize this interaction as a pure  $\sigma$ -bond that disappears as the system evolves to intermediate  $10$ . The last two columns in Table 1 display how the aromatic C(2)–H bond breaks and migrates to the benzylidene group in intermediate  $9$ , then to the metal in intermediate  $8$ , and finally migrates back to the benzylidene C atom in intermediate  $10$ .

Analysis of the aromaticity through the HOMA index of the 6-carbon rings displayed in Table 2 reveals that both the phenyl N-substituents maintain the aromaticity even in the  $5 \rightarrow 6$  step. The constantly preserved aromaticity of the phenyl ring undergoing the C–H (de)activation is key for the occurrence of this reaction, since reduction of aromaticity would imply larger energy barriers. Furthermore, the overall structure of the NHC-ligand is not distorted in any step according to the constant aromaticity of the aromatic ring formed at the backbone of this ligand. The only aromatic ring showing changes in aromaticity is the phenyl ring of the benzylidene group. This ring is fundamental to stabilize the various isomers of complex  $5$  through strong donation to the unsaturated Ru center. The HOMA index of this ring drops from 0.850 in the starting complex  $3$ , a value substantially similar to that of the other aromatic rings, to a minimum of 0.141 in  $5'$ , and rises to 0.364 and 0.455 in the crystallographically characterized products  $5$  and  $6$ . This reduction in aromaticity is of course compensated by coordination to the metal, and results in an elongation of the average C–C bond distance from 1.411 to 1.435 Å.

**Table 1**  
Mayer Bond Order (MBO) analysis of the deactivation pathway.


	Ru–C(1)	Ru–C(2)	C(1)–C(2)	C(1)–H	C(2)–H
<b>3</b>	1.675	0.000	0.000	0.000	0.958
<b>7</b>	1.623	0.004	0.000	0.000	0.978
<b>TS-7-7'</b>	1.597	0.110	0.000	0.006	0.913
<b>7'</b>	1.526	0.456	0.000	0.035	0.633
<b>TS-7'-9</b>	1.173	0.757	0.000	0.211	0.185
<b>9</b>	0.870	0.950	0.031	0.906	0.001
<b>TS-9-8</b>	1.224	0.802	0.082	0.178	0.004
<b>8</b>	1.240	0.799	0.085	0.152	0.003
<b>TS-8-10</b>	1.089	0.724	0.305	0.113	0.003
<b>10</b>	0.857	0.037	0.974	0.876	0.002
<b>TS-10-5'''</b>	0.519	0.024	0.964	0.832	0.001
<b>5'''</b>	0.332	0.035	1.056	0.867	0.027
<b>TS-5'''-5''</b>	0.071	0.013	1.085	0.887	0.034
<b>5''</b>	0.003	0.015	1.082	0.890	0.039
<b>TS-5''-5'</b>	0.001	0.014	1.075	0.889	0.039
<b>5'</b>	0.000	0.015	1.080	0.890	0.035
<b>TS-5'-5</b>	0.000	0.019	1.080	0.882	0.040
<b>5</b>	0.000	0.025	1.071	0.871	0.044
<b>TS-5-6</b>	0.000	0.019	1.069	0.871	0.043
<b>6</b>	0.000	0.015	1.068	0.874	0.042

**Table 2**  
HOMA analysis of the deactivation pathway.


	Ring 1	Ring 2	Ring 3	Ring 4
<b>3</b>	0.913	0.910	0.850	0.902
<b>7</b>	0.908	0.913	0.838	0.896
<b>TS-7-7'</b>	0.906	0.921	0.831	0.889
<b>7'</b>	0.847	0.922	0.819	0.884
<b>TS-7'-9</b>	0.879	0.917	0.816	0.880
<b>9</b>	0.868	0.915	0.803	0.874
<b>TS-9-8</b>	0.897	0.915	0.819	0.878
<b>8</b>	0.897	0.915	0.816	0.879
<b>TS-8-10</b>	0.859	0.915	0.845	0.881
<b>10</b>	0.872	0.919	0.865	0.890
<b>TS-10-5'''</b>	0.862	0.895	0.879	0.874
<b>5'''</b>	0.871	0.924	0.570	0.899
<b>TS-5'''-5''</b>	0.878	0.920	0.343	0.900
<b>5''</b>	0.895	0.913	0.141	0.896
<b>TS-5''-5'</b>	0.902	0.921	0.240	0.903
<b>5'</b>	0.897	0.915	0.457	0.894
<b>TS-5'-5</b>	0.893	0.916	0.541	0.894
<b>5</b>	0.890	0.923	0.364	0.900
<b>TS-5-6</b>	0.887	0.849	0.377	0.884
<b>6</b>	0.883	0.874	0.455	0.875

#### 4. Conclusions

In conclusion, aided by DFT calculations we have characterized the full deactivation mechanism of a second-generation Ru-based catalyst from the starting precatalyst to the experimentally determined deactivation products. In particular, we have shown that all the intermediates proposed by Grubbs and co-workers are indeed possible intermediates in the deactivation pathway, although the

sequence of steps is somewhat different from what originally proposed [7f], but confirming the presence of the Ru-hydride species **8** that was not considered in a recent mechanistic study [7m]. The inclusion of this species along the reaction pathway results in a smoother energy profile around the C–C bond formation step. Further, we have provided insights into the equilibrium between the experimental products **5** and **6**, equilibrium that is shifted towards **6** by the HCl molecule formed during the first C–H (de)activation step, that is trapped by a PCy<sub>3</sub> molecule. This is in qualitative agreement with the experimental results that indicated that species **5** could not evolve to **6** without the presence of free PCy<sub>3</sub>.

#### Acknowledgements

The research leading to these results has received funding from the European Community's Seventh Framework Programme (FP7/2007–2013) under grant agreement no. CP-FP 211468-2 EUMET. We thank ENEA (<http://www.enea.it>) and the HPC team for support as for using the ENEA-GRID and the HPC facilities CRESCO (<http://www.cresco.enea.it>) Portici (Naples), Italy and BSC (Altamira Project QCM-2009-3-0006) for access to remarkable computational resources. A.P. thanks the Generalitat de Catalunya for a Beatriu de Pinós postdoctoral contract.

#### References

- [1] R.H. Grubbs, Handbook of Olefin Metathesis, Wiley-VCH, Weinheim, Germany, 2003.
- [2] S.T. Nguyen, R.H. Grubbs, J.W. Ziller, J. Am. Chem. Soc. 115 (1993) 9858–9859.
- [3] (a) M. Scholl, S. Ding, C.W. Lee, R.H. Grubbs, Org. Lett. 1 (1999) 953–956; (b) J. Huang, E.D. Stevens, S.P. Nolan, J.L. Peterson, J. Am. Chem. Soc. 121 (1999) 2674–2678; (c) C.W. Bielawski, R.H. Grubbs, Angew. Chem., Int. Ed. 39 (2000) 2903–2906; (d) T. Weskamp, F.J. Kohl, W. Hieringer, D. Gleich, W.A. Herrmann, Angew. Chem., Int. Ed. Engl. 38 (1999) 2416–2419.
- [4] H. Jacobsen, A. Correa, A. Poater, C. Costabile, L. Cavallo, Coord. Chem. Rev. 253 (2009) 687–703 (And references therein).
- [5] (a) A.H. Hoveyda, R.R. Schrock, J. Chem. Eur. 7 (2001) 945–950; (b) R.R. Schrock, A.H. Hoveyda, Angew. Chem., Int. Ed. 42 (2003) 4592–4633;



- (c) A. Fürstner, *Angew. Chem., Int. Ed.* 39 (2000) 3012–3043;  
(d) T.M. Trnka, R.H. Grubbs, *Acc. Chem. Res.* 34 (2001) 18–29.
- [6] (a) E.L. Dias, S.T. Nguyen, R.H. Grubbs, *J. Am. Chem. Soc.* 119 (1997) 3887–3897;  
(b) M. Ulman, R.H. Grubbs, *Organometallics* 17 (1998) 2484–2489;  
(c) C. Adlhart, C. Hinderling, H. Baumann, P. Chen, *J. Am. Chem. Soc.* 122 (2000) 8204–8214;  
(d) A. Michrowska, R. Bujok, S. Harutyunyan, V. Sashuk, G. Dolgonos, K. Grela, *J. Am. Chem. Soc.* 126 (2004) 9318–9325;  
(e) K. Getty, M.U. Delgado-Jaime, P. Kennepohl, *J. Am. Chem. Soc.* 129 (2007) 15774–15776;  
(f) E.F. van der Eide, P.E. Romero, W.E. Piers, *J. Am. Chem. Soc.* 130 (2008) 4485–4491;  
(g) L. Cavallo, *J. Am. Chem. Soc.* 124 (2002) 8965–8973;  
(h) A. Correa, L. Cavallo, *J. Am. Chem. Soc.* 128 (2006) 13352–13353.
- [7] (a) R.F.R. Jazsar, S.A. Macgregor, M.F. Mahon, S.P. Richards, M.K. Whittlesey, *J. Am. Chem. Soc.* 124 (2002) 4944–4945;  
(b) D. Giunta, M. Hölscher, C.W. Lehmann, R. Mynott, C. Wirtz, W. Leitner, *Adv. Synth. Catal.* 345 (2003) 1139–1145;  
(c) K. Ab-dur-Rashid, T. Fedorkiw, A.J. Lough, R.H. Morris, *Organometallics* 23 (2004) 86–94;  
(d) R. Dorta, E.D. Stevens, S.P. Nolan, *J. Am. Chem. Soc.* 126 (2004) 5054–5055;  
(e) N.M. Scott, R. Dorta, E.D. Stevens, A. Correa, L. Cavallo, S.P. Nolan, *J. Am. Chem. Soc.* 127 (2005) 3516–3526;  
(f) S.H. Hong, A. Chlenov, M.W. Day, R.H. Grubbs, *Angew. Chem., Int. Ed.* 46 (2007) 5148–5151;  
(g) J.M. Berlin, K. Campbell, T. Ritter, T.W. Funk, A. Chlenov, R.H. Grubbs, *Org. Lett.* 9 (2007) 1339–1342;  
(h) S.H. Hong, M.W. Day, R.H. Grubbs, *J. Am. Chem. Soc.* 126 (2004) 7414–7415;  
(i) M. Ulman, R.H. Grubbs, *J. Org. Chem.* 64 (1999) 7202–7207;  
(l) S.H. Hong, A.G. Wenzel, T.T. Salguero, M.W. Day, R.H. Grubbs, *J. Am. Chem. Soc.* 129 (2007) 7961–7968;  
(m) J. Mathew, N. Koga, C.H. Suresh, *Organometallics* 27 (2008) 4666–4670.
- [8] (a) B.R. Galan, M. Gembicky, P.M. Dominiak, J.B. Keister, S.T. Diver, *J. Am. Chem. Soc.* 127 (2005) 15702–15703;  
(b) A. Poater, F. Ragone, A. Correa, L. Cavallo, *J. Am. Chem. Soc.* 131 (2009) 9000–9006;  
(c) S.T. Diver, *Coord. Chem. Rev.* 251 (2007) 671–701;  
(d) B.R. Galan, M. Pitak, M. Gembicky, J.B. Keister, S.T. Diver, *J. Am. Chem. Soc.* 131 (2009) 6822–6832.
- [9] M.J. Frisch, G.W. Trucks, H.B. Schlegel, G.E. Scuseria, M.A. Robb, J.R. Cheeseman, V.G. Zakrzewski, J.A.J. Montgomery, R.E. Stratmann, J.C. Burant, S. Dapprich, J.M. Millam, A.D. Daniels, K.N. Kudin, M.C. Strain, O. Farkas, J. Tomasi, V. Barone, M. Cossi, R. Cammi, B. Mennucci, C. Pomelli, C. Adamo, S. Clifford, J. Ochterski, G.A. Petersson, P.Y. Ayala, Q. Cui, K. Morokuma, D.K. Malick, A.D. Rabuck, K. Raghavachari, J.B. Foresman, J. Cioslowski, J.V. Ortiz, B.B. Stefanov, G. Liu, A. Liashenko, P. Piskorz, I. Komaromi, R. Gomperts, R.L. Martin, D.J. Fox, T. Keith, M.A. Al-Laham, C.Y. Peng, A. Nanayakkara, C. Gonzalez, M. Challacombe, P.M.W. Gill, B. Johnson, W. Chen, M.W. Wong, J.L. Andres, C. Gonzalez, M. Head-Gordon, E.S. Replogle, J.A. Pople, Gaussian 03, Gaussian, Inc., Pittsburgh, PA, 2003.
- [10] (a) A.D. Becke, *Phys. Rev. A* 38 (1988) 3098–3100;  
(b) J.P. Perdew, *Phys. Rev. B* 33 (1986) 8822–8824;  
(c) J.P. Perdew, *Phys. Rev. B* 34 (1986) 7406.
- [11] (a) A. Schaefer, H. Horn, R. Ahlrichs, *J. Chem. Phys.* 97 (1992) 2571–2577;  
(b) A. Schaefer, C. Huber, R. Ahlrichs, *J. Chem. Phys.* 100 (1999) 5829–5835.
- [12] (a) U. Haeusermann, M. Dolg, H. Stoll, H. Preuss, *Mol. Phys.* 78 (1993) 1211–1224;  
(b) W. Kuechle, M. Dolg, H. Stoll, H. Preuss, *J. Chem. Phys.* 100 (1994) 7535;  
(c) T. Leininger, A. Nicklass, H. Stoll, M. Dolg, P. Schwerdtfeger, *J. Chem. Phys.* 105 (1996) 1052–1059.
- [13] (a) M. Cossi, V. Barone, R. Cammi, J. Tomasi, *Chem. Phys. Lett.* 255 (1996) 327–335;  
(b) M.T. Cancès, B. Mennucci, J. Tomasi, *J. Chem. Phys.* 107 (1997) 3032–3041;  
(c) M. Cossi, V. Barone, B. Mennucci, J. Tomasi, *Chem. Phys. Lett.* 286 (1998) 253–260.
- [14] (a) I. Mayer, *Chem. Phys. Lett.* 97 (1983) 270–274;  
(b) I. Mayer, *Int. J. Quant. Chem.* 26 (1984) 151–154.
- [15] (a) A.J. Bridgeman, N. Harris, N.A. Young, *Chem. Commun.* (2000) 1241–1242;  
(b) A.J. Bridgeman, N.A. Nielsen, *Inorg. Chim. Acta* 303 (2000) 107–115;  
(c) A.J. Bridgeman, J. Rothery, *J. Chem. Soc., Dalton Trans.* (1999) 4077–4082;  
(d) A.J. Bridgeman, J. Rothery, *Inorg. Chim. Acta* 288 (1999) 17–28;  
(e) A.J. Bridgeman, *Polyhedron* 17 (1998) 2279–2288;  
(f) A.J. Bridgeman, *J. Chem. Soc., Dalton Trans.* (1997) 2887–2893;  
(g) A.J. Bridgeman, *J. Chem. Soc., Dalton Trans.* (1997) 1323–1329.
- [16] (a) A.J. Bridgeman, J. Rothery, *J. Chem. Soc., Dalton Trans.* (2000) 211–218;  
(b) A.J. Bridgeman, *J. Chem. Soc., Dalton Trans.* (1996) 2601–2607;  
(c) A.J. Bridgeman, *J. Chem. Soc., Dalton Trans.* (1997) 4765–4771;  
(d) A.J. Bridgeman, C.H. Bridgeman, *Chem. Phys. Lett.* 272 (1997) 173–177;  
(e) A.J. Bridgeman, G. Cavigliasso, L.R. Ireland, J. Rothery, *J. Chem. Soc., Dalton Trans.* (2001) 2095–2108;  
(f) A. Poater, M. Duran, P. Jaque, A. Toro-Labbé, M. Solà, *J. Phys. Chem. B* 110 (2006) 6526–6536;  
(g) A. Poater, S. Moradell, E. Pinilla, J. Poater, M. Solà, M.A. Martínez, A. Llobet, *Dalton Trans.* (2006) 1188–1196.
- [17] (a) J. Kruszewski, T.M. Krygowski, *Tetrahedron Lett.* (1972) 3839–3842;  
(b) T.M. Krygowski, *J. Chem. Inf. Comp. Sci.* 33 (1993) 70–78.
- [18] For examples of  $\eta^2$ -coordinated benzyl groups see:  
(a) F.A. Cotton, C.A. Murillo, M.A. Petrukhina, *J. Organomet. Chem.* 573 (1999) 78–86;  
(b) W. Clegg, M.R.J. Elsegood, P.W. Dyer, V.C. Gibson, E.L. Marshall, *Acta Crystallogr. C* 55 (1999) 916–918.
- [19] Attempts to find a transition state in which PCy<sub>3</sub> assists H-extraction from 5 were unsuccessful.